Title	Photoluminescence characteristics of GaInNAs quantum wells annealed at high temperature
Author(s)	Ng, T. K.; Yoon, Soon Fatt; Wang, S. Z.; Loke, Wan Khai; Fan, Weijun
Citation	Ng, T. K., Yoon, S. F., Wang, S. Z., Loke, W. K., & Fan, W. (2002). Photoluminescence characteristics of GaInNAs quantum wells annealed at high temperature. Journal of vacuum science & technology B : Microelectronics and nanometer structures, 20(3), 964.
Date	2002
URL	http://hdl.handle.net/10220/18004
Rights	

Photoluminescence characteristics of GaInNAs quantum wells annealed at high temperature

T. K. Ng, S. F. Yoon,[a] S. Z. Wang, W. K. Loke, and W. J. Fan
School of Electrical and Electronic Engineering (Block S1), Nanyang Technological University, Nanyang Avenue, Singapore 639798, Singapore

(Received 30 October 2001; accepted 18 March 2002)

The photoluminescence (PL) characteristics of GaInNAs quantum wells (QWs) after high-temperature postgrowth annealing were studied. The QWs were grown using a radio-frequency nitrogen plasma source in conjunction with a solid-source molecular-beam epitaxy system. It was found that annealing at high temperature (840 °C) and long duration (10 min) results in significant improvements to the PL characteristics of the GaInNAs QWs. The shift of the GaInNAs and GaInAs PL peak wavelength resulting from high-temperature annealing is dependent on the In composition. It is suggested that the dominant mechanisms that give rise to the blueshift of the PL peak wavelength in GaInNAs QWs with high-In composition are residual-strain-induced GaAs/GaInNAs/GaAs interface interdiffusion, and defect-assisted diffusion-related effects, both of which originate from the growth process. © *2002 American Vacuum Society.* [DOI: 10.1116/1.1477425]

I. INTRODUCTION

Small-band-gap nitride compound semiconductors, such as GaNAs and GaInNAs, are currently important materials for optoelectronic devices such as lasers operating at 1.3 and 1.55 μm. The need for high-speed data link and optical networks drives the demand for the devices. In particular, the higher characteristic temperature of GaInNAs/GaAs lasers provides an advantage over the GaInPAs/InP lasers. The GaInNAs/GaAs system has larger conduction-band discontinuity and, therefore, provides better electron confinement and characteristic temperature.[1] From an economic viewpoint, GaInNAs-based lasers use the cheaper and more robust GaAs substrate, as compared to the more expensive and fragile InP substrate used in GaInPAs-based lasers.

Previous developments using GaInNAs showed room-temperature operation of 1.3 μm GaInNAs edge-emitting lasers[2–4] and room-temperature pulsed operation of 1.18 μm GaInNAs vertical-cavity surface-emitting lasers (VCSELs).[2,5] The GaInNAs alloy has great potential for realizing long-wavelength VSCELs[6] using GaAs substrates because the readily available GaInAs/GaAs VCSEL structures can be used. However, the threshold current of these devices is generally high because of the poor optical quality of the GaInNAs active layer.[2] It is known that as-grown GaInNAs materials are relatively defective, an effect caused by the large difference in atomic sizes of Ga, In, and As atoms compared to the N atom, and bombardment of energetic nitrogen ions during growth. Postgrowth thermal treatment[7,8] is, therefore, required to anneal the defects and, hence, obtain better photoluminescence (PL) properties, which are essential for laser applications.

Although there are reports on postgrowth annealing of GaInNAs grown using metal–organic chemical-vapor deposition (MOCVD)[9–11] and chemical-beam epitaxy (CBE),[12–14] few reports exist on high-temperature (>800 °C) treatment of this material grown by a radio-frequency (rf) nitrogen plasma source in conjunction with solid-source molecular-beam epitaxy (SSMBE). High-temperature treatment of the GaInNAs material is essential to improve its quality. Pan *et al.*[15] reported that annealing at a different temperature range results in the removal of defects of different natures in GaInNAs materials with the same In composition and grown by a dc-activated nitrogen plasma source. Only high-temperature annealing (>800 °C) could remove both defects originating from the GaAs/GaInNAs/GaAs interfaces (caused by nitrogen-ion-induced damage) and the GaInNAs layer (caused by insufficient surface migration of In and Ga atoms during growth). On the other hand, low-temperature annealing (650 °C) could only remove defects caused by nitrogen-ion-induced damage originating from the GaAs/GaInNAs/GaAs interfaces. The end result is a smaller wavelength shift (<10 nm) after low-temperature (650 °C) annealing (LTA) and a greater wavelength shift (~30 nm) after high-temperature (>800 °C) annealing (HTA).

In order to clarify the mechanisms of the large PL wavelength shift in GaInNAs after high-temperature annealing, we investigate the PL properties of GaInNAs quantum wells (QWs) with different indium compositions after a 10 min high-temperature (840 °C) postgrowth thermal annealing cycle. The mechanisms that influence the large PL wavelength shift of GaInNAs after high-temperature annealing, which were found to be dependent on the In composition, are described.

II. EXPERIMENTAL DETAILS

The GaInNAs samples were grown on semi-insulating GaAs(100) substrates using a SSMBE system equipped with a rf nitrogen plasma source. A turbomolecular pump was used to enhance the pumping capability in addition to the standard ion pump. Prior to growth, surface oxide desorption was carried out under As_4 flux at a beam-equivalent pressure

[a]Electronic mail: esfyoon@ntu.edu.sg

(BEP) of 4.5×10^{-6} Torr. The surface oxide was desorbed by slowly ramping up the substrate temperature until the reflection high-energy electron diffraction (RHEED) pattern showed a clear and abrupt transformation to (2×4) surface reconstruction. This surface reconstruction was adopted as a mean for calibrating the substrate temperature (T_s), which was measured using an infrared pyrometer of suitable wavelength sensitivity.

Ultra-high-purity nitrogen gas is admitted into the plasma source and excited by a rf power supply to generate the nitrogen radicals for the GaInNAs growth. The rf power was fixed at 450 W and the nitrogen gas flow rate was fixed at 0.1 sccm. This gives a background pressure of 3.5×10^{-6} Torr. The Ga and In fluxes were supplied from standard effusion cells. Samples A and B were grown with In BEP of 2.1×10^{-7} and 2.8×10^{-7} Torr, respectively. The Ga BEP was fixed at 4.6×10^{-7} Torr throughout the growth process. In order to maintain a smooth growth front essential for high-quality material, the As overpressure was maintained at a BEP of 4.6×10^{-6} Torr throughout the growth process. The GaInAs layer was grown to serve as a reference for determining the In composition[16] and comparison of the PL spectrum.

The sample structure consists of a GaInNAs quantum well grown above a GaAs buffer layer followed by a GaInAs QW. A GaAs barrier layer was grown between the two QWs and a GaAs cap layer was grown at top of the sample. The nominal thickness of the GaInNAs and GaInAs QWs was 6 nm. Details of the sample structures are tabulated in Table I. The corresponding PL characteristics are shown in Table II.

The samples were subjected to postgrowth thermal annealing in a system heated by an array of upper and lower lamps under nitrogen flow. The annealing temperature was fixed at 840 °C for 10 min. The sample was capped with a GaAs wafer during annealing to prevent arsenic loss at elevated temperatures. The PL measurements at 4 K were carried out using the 514.5 nm line of an Ar-ion laser. A liquid-nitrogen-cooled Ge detector in conjunction with a standard lock-in technique was used to detect the PL emission. The PL intensities of all samples were normalized to the same incident power (250 mW) to enable direct comparison between the results.

TABLE I. Growth details of the samples under study.

Details	Sample A	Sample B
GaAs Cap thickness (nm)	80	80
$Ga_{1-y}In_yAs$ thickness (nm)	6	6
GaAs barrier thickness (nm)	100	100
$Ga_{1-y}In_yN_xAs_{1-x}$ thickness (nm)	6	6
GaAs buffer thickness (nm)	300	300
Growth temperature (°C)	480	480
In beam-equivalent pressure (Torr)	2.1×10^{-7}	2.8×10^{-7}

III. RESULTS AND DISCUSSION

In Figs. 1(a) and 1(b), the solid and dotted lines indicate the PL spectrum (at 4 K) of samples A and B before annealing (as grown) and after annealing at 840 °C for 10 min, respectively. The GaInAs quantum well in sample A has lower In composition ($y=22\%$) compared to that in sample B ($y=30\%$). Therefore, the as-grown GaInAs QW in sample A emits PL at a shorter wavelength (950.5 nm) compared to that in sample B (1021 nm). Due to the higher growth rate in sample B, caused by the greater In flux during growth, the amount of nitrogen incorporated in the sample B GaInNAs layer is reduced. Hence, this results in a smaller difference between the PL peak wavelength positions of the as-grown GaInAs and GaInNAs QWs in sample B ($\Delta\lambda_{B,\text{as-grown}}=80$ nm) compared to that in sample A

TABLE II. Effects of thermal annealing on the (a) PL peak wavelength, (b) FWHM, and (c) PL peak wavelength blueshift of GaInNAs and GaInAs quantum wells.

(a) PL peak wavelength (nm)

	Before annealing		After annealing	
Sample	GaInNAs QW	GaInAs QW	GaInNAs QW	GaInAs QW
A	1093	950.5	1021	941
B	1101.5	1021	1014.5	962

(b) FWHM (meV)

	Before annealing		After annealing	
Sample	GaInNAs QW	GaInAs QW	GaInNAs QW	GaInAs QW
A	63.1	7.8	16.3	7.2
B	23.2	14.5	14	8.4

(c) PL peak wavelength blueshift (nm)

Sample	GaInNAs QW	GaInAs QW
A	$\Delta\lambda_{A,GaInNAs}=70$	$\Delta\lambda_{A,GaInAs}=10$
B	$\Delta\lambda_{B,GaInNAs}=87$	$\Delta\lambda_{B,GaInAs}=60$

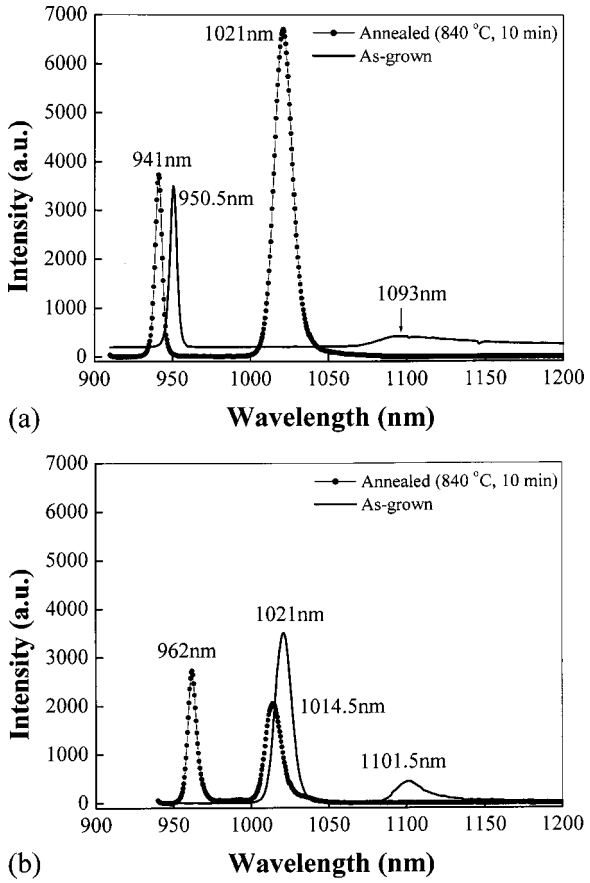

FIG. 1. Comparison of PL (4 K) intensity vs wavelength before (as grown) and after annealing for (a) sample A and (b) sample B.

($\Delta\lambda_{A,\text{as-grown}}=143$ nm). The nitrogen content, which was estimated by QW calculations,[16] in samples A and B was estimated to be $\sim 1.2\%$ and $\sim 0.6\%$, respectively.

In Fig. 1(a), the as-grown GaInAs QW exhibits a high intensity (3500 a.u.) at 950.5 nm with a full width at half maximum (FWHM) of 7.8 eV. However, the as-grown GaInNAs QW exhibits relatively poor PL emission (at ~ 1093 nm), indicating the presence of defective material. Thermal annealing at 840 °C for 10 min results in a significant increase in PL emission intensity (at ~ 1021 nm) from the GaInNAs QW by 30 times (to 6700 a.u.) and reduction in the FHWM from 63.1 to 16.3 meV. This improvement is comparable to results reported in the existing literature.[17,18]

This indicates that high-temperature postgrowth thermal annealing has a dramatic effect on improving the optical quality of the GaInNAs QW. The high-temperature thermal annealing also has a beneficial effect on the optical quality of the GaInAs QW, which is evident from the slight reduction in the FWHM from 7.8 meV (before annealing) to 7.2 meV (after annealing). The results of the FWHM change in samples A and B arising from the thermal annealing are summarized in Table II(b).

Pan *et al.*[15] have previously reported improvement in the GaInAs and GaInNAs QW optical quality arising from thermal annealing. They studied the mechanisms for GaInNAs quality improvement by applying high- and low-temperature annealing to three samples of the same In composition, but prepared under different applied magnetic fields to the plasma. The magnetic field, which is applied perpendicular to the path of the nitrogen-ion plasma flux, served to deflect the ion flux. The deflection effect is stronger at higher magnetic field, and therefore, fewer defects due to nitrogen-ion-induced damage were created. Such samples showed a less significant change in PL properties after LTA, due to the presence of fewer defects. In addition, the wavelength shift after LTA was attributed by Pan *et al.*[15] to Ga and In diffusion at the GaAs/GaInNAs/GaAs interfaces, rather than N–As diffusion.

The Pan *et al.* study[15] also showed that HTA results in removal of defects caused by insufficient surface migration of Ga and In at low growth temperature and removal of nitrogen-ion-induced defects. The wavelength shift after HTA was attributed to N–As and Ga and In diffusion. As the GaInNAs peak PL intensities increased rapidly in the beginning of HTA and reached a maximum in 5 s, it is also suggested that N–As diffusion is dominant at the beginning of the HTA process when nitrogen-ion-induced defects are plenty, and Ga and In diffusion is dominant after most of the defects are removed.[15,19]

The results from our annealing study on two GaAs/GaInAs/GaAs/GaInNAs/GaAs samples with different In compositions are consistent with the above. The defects resulted from nitrogen-ion-induced damage and insufficient surface migration of Ga and In atoms during low-temperature growth were removed, as evident from the increase in PL intensity of the GaInAs emission peak as shown in Fig. 1(a). Therefore, the annealing temperature of 840 °C used in our study should have the effect of eliminating defects resulting from nitrogen-ion-induced damage, as well as defects resulting from insufficient Ga and In surface migration during low-temperature growth, as reported by Pan *et al.*[15] The GaInNAs QW in sample A clearly shows significantly higher PL intensity [Fig. 1(a)] and smaller FWHM [Table II(b)] as a result of the annealing process.

To understand the mechanism of the PL peak wavelength shift after thermal annealing, we first examined the GaInAs QW. The effect of GaAs/GaInNAs/GaAs interface diffusion of the host atoms (Ga and In) is shown in Fig. 1(a), where the PL position of the GaInAs emission peak (sample A) has shifted downwards from 950.5 to 941 nm after annealing (a change in wavelength of $\Delta\lambda_{A,\text{GaInAs}}=10$ nm). The relatively defective as-grown GaInNAs material exhibits a larger wavelength shift of $\Delta\lambda_{A,\text{GaInNAs}}=70$ nm (from 1093 to 1021 nm) after annealing, due to In and Ga interdiffusion as well as nitrogen-ion-damage defect-assisted diffusion at the GaAs/GaInNAs/GaAs interfaces. As for sample B [Fig. 1(b)], the PL peak wavelength position of GaInAs emission has shifted from 1021 nm to the lower wavelength of 962 nm after annealing, and that of GaInNAs has shifted from 1101.5 to 1014.5 nm. The change in peak wavelength of the GaInAs QW in sample B ($\Delta\lambda_{B,\text{GaInAs}}=60$ nm) is significantly larger than that in sample A ($\Delta\lambda_{A,\text{GaInAs}}=10$ nm). The results of

the PL wavelength shift in samples A and B arising from the annealing are tabulated in Table II(c).

As the annealing conditions for both samples A and B are the same, and both samples were grown under nominally identical conditions with the exception of the In flux, the mechanism that contributes to the observed large PL wavelength shift could not be caused by the difference in annealing temperature (as studied by Pan *et al.*), but rather it is caused by the difference in In composition. We suggest that the higher-In composition in sample B has contributed to the greater $\Delta\lambda_{B,GaInNAs}$ after annealing, due to the residual-strain-induced interdiffusion[20] and defect-induced interdiffusion as a result of In incorporation. As the In composition in sample B is higher, more severe residual-strain-induced interdiffusion of Ga and In atoms at the GaAs/GaInAs/GaAs interfaces may occur.

However, such effects are lower in sample A due to its lower-In composition. Also, the argument of defect-assisted interdiffusion in the GaInAs QW during annealing is supported by the lower crystal quality of the as-grown GaInAs in sample B as observed in the PL FWHM [see Table II(b)]. The as-grown GaInAs PL FWHM of 14.5 meV in sample B is larger than that of the as-grown GaInAs QW in sample A (7.8 meV). This correlates well with the reflection high-energy electron diffraction observation during growth. The time required for sample B (with higher-In composition) to transform from streaky (2×4) surface reconstruction to disjointed streak (2×1) surface reconstruction during the initial stage of GaInAs QW growth was significantly shorter than that of sample A. The RHEED observation shows that three-dimensional (3D) growth as a result of surface strain occurred earlier in sample B than in sample A. It is possible that the 3D growth results in a higher number of defects in sample B compared to sample A.

Following the above argument of residual-strain-induced interface interdiffusion and defect-assisted diffusion in the GaInAs QW, it is to be expected that the GaInNAs QW in sample B would show a larger PL wavelength shift compared to sample A. This is seen in Table II(c), where the wavelength shift of the GaInNAs QW in sample B before and after annealing ($\Delta\lambda_{B,GaInNAs}=87$ nm) is larger than that in sample A ($\Delta\lambda_{A,GaInNAs}=70$ nm). Because the GaInNAs QW in sample B has lower nitrogen content compared to sample A, the defect density related to energetic nitrogen-ion bombardment should be lower than that in sample A. This is evident in Fig. 1, where the intensity and FWHM of the as-grown GaInNAs QW in sample B are higher and lower, respectively, than those in sample A.

Therefore, the effect of nitrogen-ion-damage defect-assisted N–As diffusion and PL wavelength shift contributed by this effect in the sample B GaInNAs QW should be lower than that in sample A. However, because $\Delta\lambda_{B,GaInNAs}$ (87 nm) is larger than $\Delta\lambda_{A,GaInNAs}$ (70 nm), the residual-strain-induced GaAs/GaInNAs/GaAs interface interdiffusion and defect-induced diffusion are considered to be the dominant effects that contributed to the large PL wavelength shift of the GaInNAs QW in sample B. Therefore, this indicates that nitrogen-ion-damage defect-assisted N–As diffusion is more dominant in the GaInNAs QW with low-In content, while residual-strain-induced interdiffusion and defect-induced diffusion are more dominant at high-In composition.

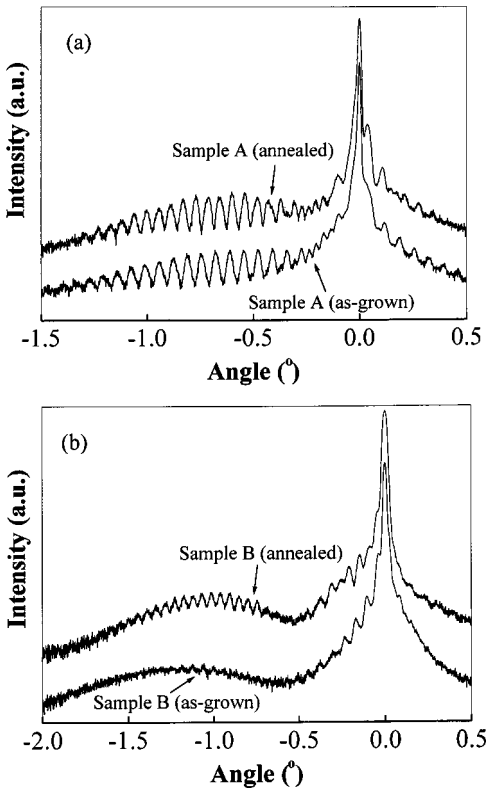

FIG. 2. Comparison of XRD scan in the (004) plane before (as grown) and after annealing for (a) sample A and (b) sample B.

The x-ray diffraction (XRD) scans in the (004) plane were used to investigate the structural change in samples A and B before and after thermal annealing. In Figs. 2(a) and 2(b), the broad humps along the negative-angle region of the x-ray spectrum increase in intensity and shift towards the substrate peak after annealing. The shifting of the broad humps is more obvious in the spectrum of sample B [Fig. 2(b)] compared to that of sample A [Fig. 2(a)], indicating greater change in the In composition in sample B. The calculated strain[21] in the GaInNAs layers for samples A and B are -0.013 and -0.020, respectively. The negative sign indicates the GaInNAs layers are compressively strained. The results show that the GaInNAs layer strain in sample B is greater than that in sample A. This further supports the above argument of residual-strain-induced PL wavelength shift.

In addition, very clear and high peak-to-peak intensities of the Pendellosung fringes on the humps were observed in the spectrum of the as-grown and annealed sample A [Fig. 2(a)], indicating the presence of abrupt layer interfaces and good crystalline quality before and after annealing. The lower peak-to-peak intensities of the Pendellosung fringes in Fig. 2(b) indicate that the layer interfaces are less well defined in sample B, and this could possibly be a source of defects at the interfaces. This is consistent with the PL FWHM observations discussed earlier and further supports

the defect-assisted interdiffusion effect that partly contributes to the large PL wavelength shift in GaInAs and GaInNAs QW emission.

IV. CONCLUSIONS

This article reports the effect of high-temperature post-growth thermal annealing on GaInAs and GaInNAs QWs grown by a rf nitrogen plasma source in SSMBE. We found that annealing at 840 °C for 10 min significantly improves the GaInNAs QW quality. This improvement was due to the annealing of nitrogen-ion-induced damage defects through defect-assisted N–As interdiffusion and the enhancement of Ga and In atom GaAs/GaInNAs/GaAs interface interdiffusion at high temperature. The blueshift of the PL peak wavelength of the GaInNAs and GaInAs emission was found to be dependent on the In composition. The dominant mechanisms contributing to the blueshift of the PL peak wavelength of the GaInNAs QW with high-In composition are residual-strain-induced GaAs/GaInNAs/GaAs interface interdiffusion and defect-assisted diffusion. However, for the GaInNAs QW with low-In composition, the nitrogen-ion damage-assisted N–As interdiffusion effect at the GaAs/GaInNAs/GaAs interfaces dominates. The results are supported by evidence from PL and XRD measurements, as well as RHEED observation.

ACKNOWLEDGMENTS

One of the authors (T.K.N.) wishes to express his sincere appreciation to Zheng Haiqun and Dr. Sun Zhongzhe for their assistance during the start up of the rf nitrogen plasma source.

[1]M. Kondow, K. Uomi, A. Niwa, T. Kitatani, S. Watahiki, and Y. Yazawa, Jpn. J. Appl. Phys., Part 1 **35**, 1273 (1996).
[2]T. Kageyama, T. Miyamoto, S. Makino, F. Koyama, and K. Iga, Jpn. J. Appl. Phys., Part 2 **38**, L298 (1999).
[3]K. Nakahara, M. Kondow, T. Kitatani, M. C. Larson, and K. Uomi, IEEE Photonics Technol. Lett. **10**, 487 (1998).
[4]S. Sato, Y. Osawa, T. Saitoh, and I. Fujimura, Electron. Lett. **33**, 1386 (1997).
[5]M. C. Larson, M. Kondow, T. Kitatani, K. Nakahara, K. Tamura, H. Inoue, and K. Uomi, IEEE Photonics Technol. Lett. **10**, 188 (1998).
[6]K. Iga, Proceedings of the InP and Related Materials Conference (IPRM'96), 1996, ThA1-1.
[7]X. Yang, J. B. Heroux, M. J. Jurkovic, and W. I. Wang, J. Vac. Sci. Technol. B **17**, 1144 (1999).
[8]L. Largeau, C. Bondoux, G. Patriarche, C. Asplund, A. Fujioka, F. Salomonsson, and M. Hammar, Appl. Phys. Lett. **79**, 1795 (2001).
[9]S. Tanaka, A. Moto, T. Tanabe, N. Ikoma, and S. Takagishi, Extended Abstracts (45th Spring Meeting, 1998), Japan Society of Applied Physics and Related Societies, p. 290.
[10]H. Saito, T. Makimoto, and N. Kobayashi, Extended Abstracts (45th Spring Meeting 1998), Japan Society of Applied Physics and Related Societies, p. 291.
[11]Z. Pan, T. Miyamoto, D. Schlenker, F. Koyama, and K. Iga, Proceedings of the InP and Related Materials Conference (IPRM'98), 1998, TuP-16.
[12]T. Miyamoto, K. Takeuchi, T. Kageyama, F. Koyama, and K. Iga, Jpn. J. Appl. Phys., Part 1 **37**, 90 (1998).
[13]K. Takeuchi, T. Miyamoto, T. Kageyama, F. Koyama, and K. Iga, Jpn. J. Appl. Phys., Part 1 **37**, 1603 (1998).
[14]T. Miyamoto, K. Takeuchi, T. Kageyama, F. Koyama, and K. Iga, J. Cryst. Growth **197**, 67 (1999).
[15]Z. Pan, L. H. Li, W. Zhang, Y. W. Lin, R. H. Wu, and W. Ge, Appl. Phys. Lett. **77**(9), 1280 (2000).
[16]S. Z. Wang (unpublished).
[17]R. A. Mair, J. Y. Lin, H. X. Jiang, E. D. Jones, A. A. Allerman, and S. R. Kurtz, Appl. Phys. Lett. **76**, 188 (2000).
[18]I. A. Buyanova, W. M. Chen, and B. Monemar, MRS Internet J. Nitride Semicond. Res. **6**, 2 (2001).
[19]Z. Pan, T. Miyamoto, S. Sato, F. Koyama, and K. Iga, Jpn. J. Appl. Phys., Part 1 **38**, 1012 (1999).
[20]S. W. Ryu, I. Kim, B. D. Choe, and W. G. Jeong, Appl. Phys. Lett. **67**, 1417 (1995).
[21]W. J. Fan and S. F. Yoon, J. Appl. Phys. **90**, 843 (2001).